

Measurement Errors from Internal Shear Strain within Fiber-Bragg-Grating Sensors

Mathias S. Müller, Thorbjörn C. Buck, Hala J. El-Khozondar and Alexander W. Koch

Technische Universität München
Institute for Measurement Systems and Sensor Technology
Theresienstr. 90, 80333 Munich, Germany

ABSTRACT

Fiber-Bragg-grating (FBG) sensors have become commercially available sensors for the measurement of temperature, strain and many other quantities. The sensor information is encoded in the spectral reflection characteristic of these devices. Their usage as strain sensors is one of the most prominent fields of application. Strains from a structure which is to be monitored are transferred into the fiber-Bragg-grating, by surface bonding or embedding. In general an arbitrary state of strain may thus occur within the FBG, represented by a full strain tensor with normal strain components, as well as with shear strain components. The influence of normal strains is well understood and has been treated theoretically by many authors. The influence of shear strains is however not well understood. As we were recently able to theoretically demonstrate by a full tensor coupled mode analysis, shear strains do influence the spectral response of fiber-Bragg-sensors and thus have to be considered. In this work, an introduction to the modeling of shear strains within fiber-Bragg-gratings is given. We discuss reasonable approximations for the simplification of the theoretical model. We compute, to our knowledge for the first time, the direct influence of shear strains on the output of a FBG measurement system and show the cases when shear strain effects are relevant. Furthermore, we compare the sensitivity of different interrogation algorithms towards shear strain influences on the measurement system output.

Keywords: fiber Bragg grating, fiber-optic sensors, measurement error, shear strain

1. INTRODUCTION

Fiber Bragg gratings (FBGs) have been considered for numerous sensing applications including temperature, strain and force among others. One intriguing aspect is the possibility to extract two parameters from the sensor position by using a polarization sensitive interrogation scheme. FBGs may be integrated into composite materials or concrete¹ due to their small dimensions. This possibility has gained much interest, because reconstruction of the state of strain within such materials may improve application such as condition monitoring.

A transversally loaded or embedded fiber Bragg grating will give an optical response corresponding to the strains that are distributed along the core of the fiber at the position of the sensor. This is due to the fact, that light is only guided close to the fiber core, which is only around ten micron in diameter, whereas the whole fiber measures approximately 100 μm . This approximation is called "center strain approximation"² and greatly simplifies the computation of the optical response of the FBG, since transversal gradients in the strain field may be neglected. The loads applied to the fiber, either by transversal loading¹⁹ or by embedding into a host material that is itself strained, as pictured in figure 1 will result in a position dependant strain field within the fiber, represented by the strain tensor $\bar{e}_f(x, y, z)$. Since the dominant contribution to the change in the optical response of the FBG will result from the core of the fiber we assume $\bar{e}_c(z) = \bar{e}_f(0, 0, z)$. The optical response of the grating upon this load is computed from coupled mode theory (CMT). CMT is a widely employed tool and has been applied to fiber Bragg gratings in various articles, see for example^{3,4}.

The influencing quantity $\bar{e}_c(z)$ is a tensor of second rank. It will, to first order produce a dielectric perturbation in the fiber, which is also represented by a second rank tensor, namely the dielectric perturbation tensor $\Delta\bar{e}$.⁵ Each of the perturbation tensor's entries may be nonzero in an arbitrary load case. We recently demonstrated, how the optical response of fiber Bragg gratings may be computed from the knowledge of this perturbation tensor by a full tensorial coupled mode theory⁶ and derived a transfer matrix formalism for the problem.⁷

The electromagnetic problem considers the four propagation modes of the fiber, two of orthogonal polarization p and s , propagating in positive z -direction and two propagating in negative z -direction. The amplitudes of these four modes A_{p+} , A_{s+} , A_{p-} and A_{s-} are coupled by the dielectric perturbations induced by the grating and the mechanical loads. In a polarization maintaining fiber, the propagation constants of the mode having orthogonal polarization $\beta_{p/s}$ differ by a value $\Delta\beta = 2\pi/L_B$, where L_B is called the beat length of the fiber.¹⁸ This difference in propagation constant will prevent the coupling of the polarization modes when the fiber is mechanically loaded, such as by twists or bends or other loads^{8,9} However, this only works for moderate loads, and polarization coupling takes place, when the fiber is substantially loaded.

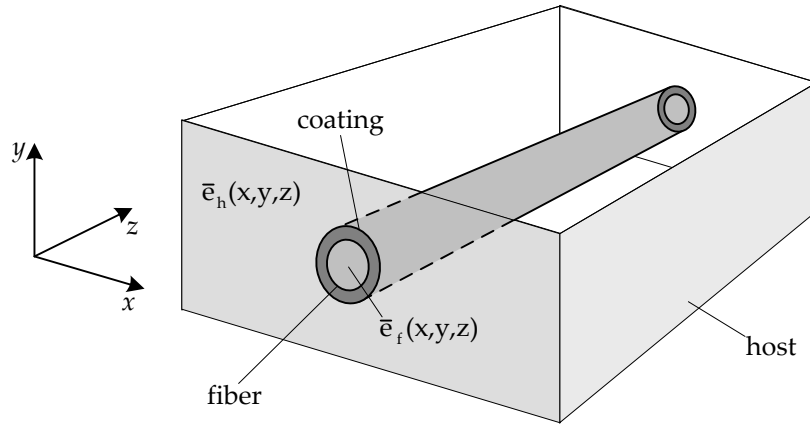


Figure 1. Optical fiber with coating embedded into a host structure. The strains in the host $\bar{e}_h(x, y, z)$ will result in strains within the optical fiber $\bar{e}_f(x, y, z)$.

When polarization mode coupling is neglected, the two orthogonal polarizations may be used to measure two different parameters from the FBGs position.^{10,11,20} Then, only the three normal strains e_{xx} , e_{yy} , e_{zz} and the temperature T have an influence on the optical response of the FBG. If all parameters are applied homogeneously along the length L of the grating, the Bragg reflection peaks of the two polarization axes will shift, without deforming their shape. The center wavelength of the two Bragg peaks is computed and from it, for example the two normal strain entries e_{xx} and e_{yy} in the strain tensor may be reconstructed. The center wavelength is obtained by using algorithms such as maximum search, a centroid algorithm¹² or gaussian fit.¹³

This is only possible, if the two other parameters, for example e_{xx} and T stay constant, which is not necessarily satisfied in every application. A solution to this has been suggested by E. Udd giving an overview in.¹⁴ The suggestion is to fabricate two Bragg gratings at the same position inside the fiber, with strongly different wavelengths (1300 nm and 1500 nm). The fiber needs to be single mode in both wavelengths. If the material properties of the fiber (Pockel's coefficients and thermo-optic coefficient) are different at both wavelengths, then it is possible to measure all four influencing quantities with one sensor. In a recent work by Mawatari¹⁵ this suggestion is investigated. The authors note the necessity of being able to neglect polarization rotation within the fiber, due to its polarization holding capabilities. They state that the problem of reconstructing the four parameters would become much more complicated, if such a polarization mode coupling would occur.

It is the aim of our work, to study the influence of polarization mode coupling within fiber Bragg gratings on the basis of the theory presented in.⁶ We give a short summary on the theory and introduce the measurement setup we model with our simulations. We show, how the parameter "shear strain", which has been widely ignored in the discussions on multiparameter strain sensing has a significant influence on the response of such a sensor. For this purpose, we simulate the reflection spectrum of a mechanically loaded FBG sensor, when shear strain is neglected and when shear strain effects are considered and compare the results. Furthermore, we calculate the performance of three different peak fitting algorithms namely maximum search, centroid and Gaussian fit.

2. FUNDAMENTALS AND MODELING

Several FBG interrogation schemes have been proposed to date. For the polarization sensitive interrogation, a polarization independent measurement is conducted and the two Bragg peaks are separated by an algorithm¹⁵ or the polarization spectra are recorded independently.^{16,17} We model the latter setup, which is pictured in figure 2. We assume, that polarized light, with an angle of 45° with respect to the axes of the polarization maintaining fiber is used to illuminate the Bragg grating. The two polarization spectra are split up by a polarization splitter and are directed to two polarization independent optical spectrum analyzers.

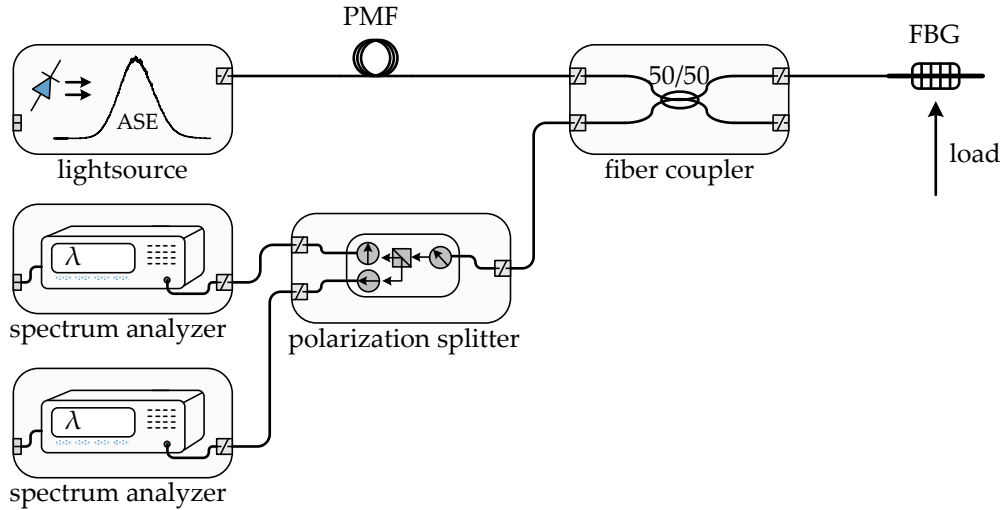


Figure 2. Possible measurement setup for determining the spectral response of a fiber Bragg grating written in a polarization maintaining fiber. The fiber Bragg grating is illuminated by a well polarized source. Both axes of the polarization maintaining fiber are illuminated equally. The reflected spectra are directed to a polarization splitter by a 3 dB fiber coupler. The polarization splitter splits the light in the fast and the slow polarization axis of the fiber. Both outputs are fed to two optical spectrum analyzers with low polarization dependency.

In a real world application, the strain tensor entries may vary independently of each other, giving a large range of parameters. In the transversal loading experiments¹⁵⁻¹⁷ this range of parameters is reduced, since only two parameters, namely the load angle ϕ and the load force F are varied. This results in a strain tensor \bar{e}_c that may be approximated by the form⁶

$$\bar{e}_c(\phi) = F \cdot R(\phi) \begin{pmatrix} e_{xx} & 0 & 0 \\ 0 & -me_{xx} & 0 \\ 0 & 0 & 0 \end{pmatrix} \cdot R(\phi)^T, \quad (1)$$

where $R(\phi)$ is the rotation matrix around the z-axis. By rotating the fiber in the experiment, the shear strain e_{xy} is generated, which possesses a maximum value of roughly that of e_{xx} .

To further simplify the model, we restrict our selves to the following load case: The only nonzero strain tensor entries are e_{xx} , $e_{yy} = -me_{xx}$ and e_{xy} . Entry e_{xx} is varied from zero to 2000 $\mu\text{m}/\text{m}$, e_{yy} is scaled with $m = 0.2$, and e_{xy} is either zero, when neglecting shear strain effects of possesses a value of $e_{xy} = 2000 \mu\text{m}/\text{m}$. These parameters may very well be found in a real application. From the spectral information, the "Bragg-wavelength" has to be extracted. Therefor several algorithms have been used. For a symmetrical Bragg peak, the algorithms - peak maximum, centroid and gaussian fit yield the same value. If the Bragg peak becomes unsymmetrical, the outputs of these algorithms will show differences. We apply the three algorithms to the two polarization mode reflections separately.

3. RESULTS AND DISCUSSION

The first load case is computed to illustrate in detail the influence of shear strain on the reflection spectra. A normal strain $e_{xx} = 2000 \mu\text{m}/\text{m}$ and $e_{xy} = 2000 \mu\text{m}/\text{m}$ is used. Figure 3 shows the computed result neglecting shear strain and taking into account shear strain.

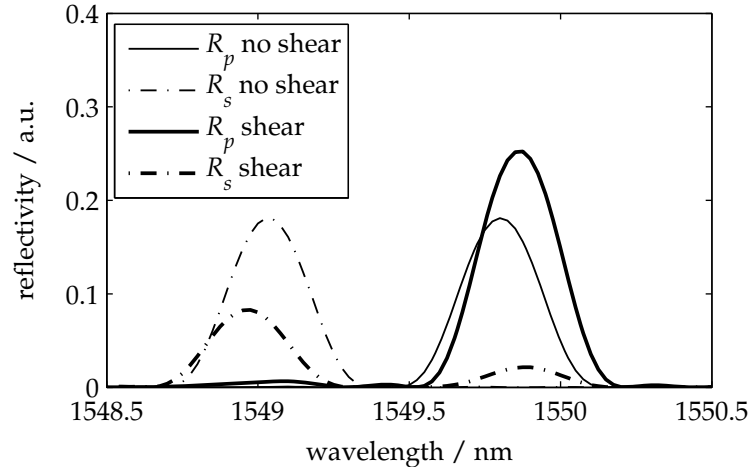


Figure 3. Result of the simulation using a normal strain $e_{xx} = 2000 \mu\text{m}/\text{m}$ and $e_{yy} = -me_{xx}$, $m = 0.2$. The shear strain is neglected in the thin lined result and set to $2000 \mu\text{m}/\text{m}$ for the simulation with shear strain. The results without shear strain show the expected shift of the spectral response, without changing the shape of the spectrum. With shear strain, the polarization modes couple and the reflection spectra are changed in shape.

As may be seen from the results neglecting shear strain, the spectral shapes of both Bragg peaks are symmetric. They shift by some amount according to the load, but do not change their spectral characteristic. The reflection spectra considering shear strain do change their characteristic. The left peak, corresponding to the s -polarization couples intensity into the right peak, corresponding to the p -polarization. This would by itself not change the output of the peak finding algorithms. But what may also be observed, is that the shear strain changes the spectral position of the peaks, something that would yield a different result. Apart from that, a second order effect may be observed, when taking a look at the s -mode's intensity at the position of the p -mode's reflection peak. There, due to polarization mode coupling, the backward propagating p -mode couples onto the backward propagating s -mode. This leads to a second peak in the s -mode spectrum, something that has been observed by Ye et al.¹⁷ in their lateral loading experiment attributing it to structural changes in the polarization maintaining fiber.

To get a further impression of the effect, the reflection spectra of the Bragg grating are computed for increasing load $e_{xx} = \{0, 400, 800, 1200, 1600, 2000\} \mu\text{m}/\text{m}$ and e_{yy} accordingly, see figure 4. e_{xy} is fixed to $2000 \mu\text{m}/\text{m}$. For low e_{xx} , the two peaks are only separated by the fiber's birefringence and the polarization modes couple strongly. This results in a s -mode reflection peak, that nearly possesses two equally strong maxims. For increasing normal strain, the separation of the polarization modes reflection peaks increases, and the the propagation constant difference increases, leading to lower polarization mode coupling. Hence, the second maxima in the s - mode reflection decreases.

Calculating the response of the interrogation algorithms we use the loads described before. We compute the output of the measurement setup for two different kind of fibers. Because polarization mode coupling will increase with increasing beat length L_B , we use the beat length values of 7.7 mm and 3.0 mm. These fibers are commercially available and represent the lower end of available fibers. Thus, polarization mode coupling is generally low in the selected fibers and effects may be expected to increase with higher beat lengths.

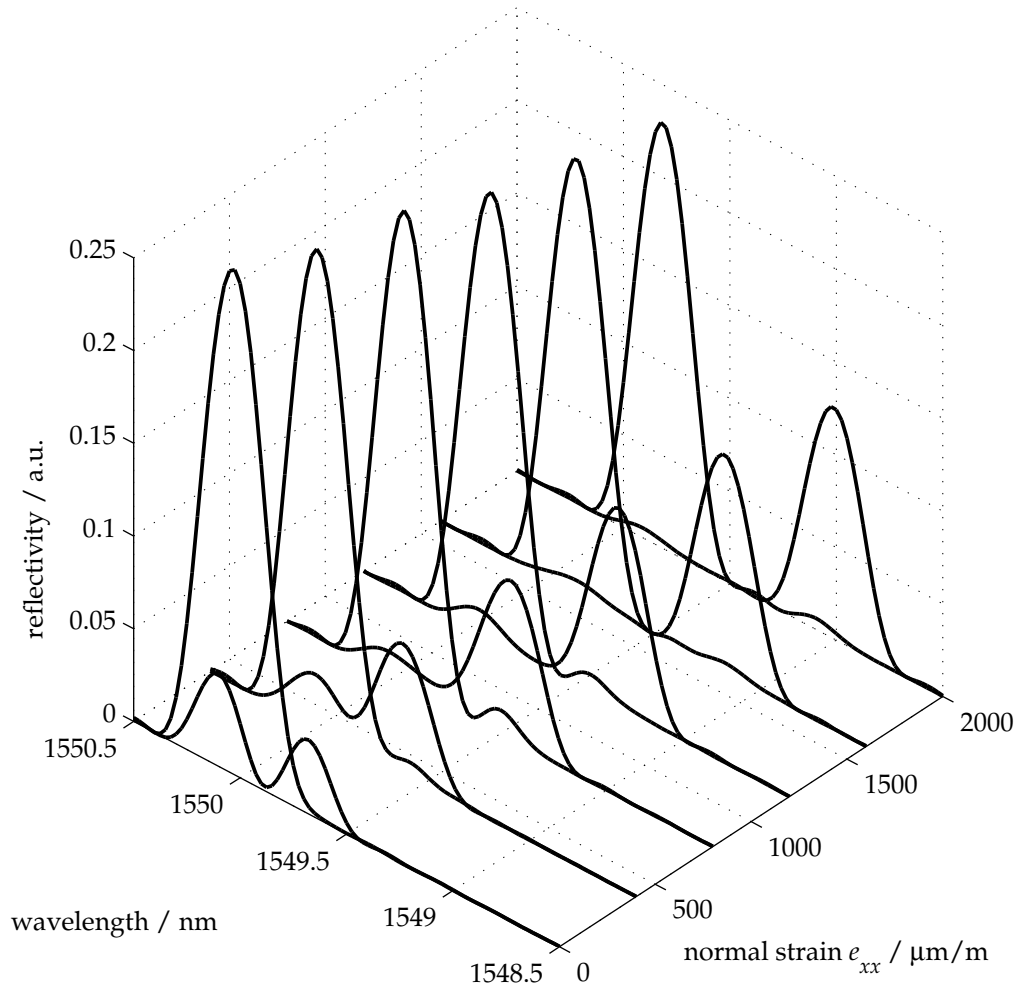


Figure 4. Six simulations with increasing normal strain and a fixed shear strain of $e_{xy} = 2000 \mu\text{m}/\text{m}$. For low normal strains, the reflection peaks are only separated by the birefringence of the fiber and polarization mode coupling is high, leading to a strong second peak in the s -mode reflection spectrum. For higher normal strain loads, the peaks separate further and polarization mode coupling is reduced.

The upper plot in figure 5 shows the results for the $L_B = 7.7 \text{ mm}$. The lower values correspond to the Bragg wavelength of the s -mode reflection spectrum, those at higher wavelengths to the p -mode reflection. The p -mode's spectral response is less deformed in shape than the s -mode. This is simply determined by the positive sign of the shear strain, using a negative value, the p -mode would be deformed in a comparable way. It may be observed, that the values for the p -mode Bragg-wavelength are all situated at higher wavelengths than without shear strain. This is something that may be explained by the spectral shift to higher values given in figure 3. Yet, the s -modes results show positive as well as negative differences. This may be explained as follows:

The maximum of the s -modes Bragg peak is at lower wavelengths than without shear strain. This will also give lower values for the maximum algorithm. The Gaussian fit will fit to the strong left peak of the s -mode in figure 3, but the centroid algorithm will integrate over the whole spectrum, and weighting it with the spectral position. This will give the right second peak in the s -modes reflection spectrum a special influence on the position of the Bragg-wavelength. For low normal strains, the polarization mode coupling is strongest, leading to a strong second peak in the s -modes reflection spectrum. The Gaussian fit algorithm will either fit to one or the other, yielding strong deviations.

If the beat length is decreased viz. the birefringence of the fiber is higher, the polarization mode coupling

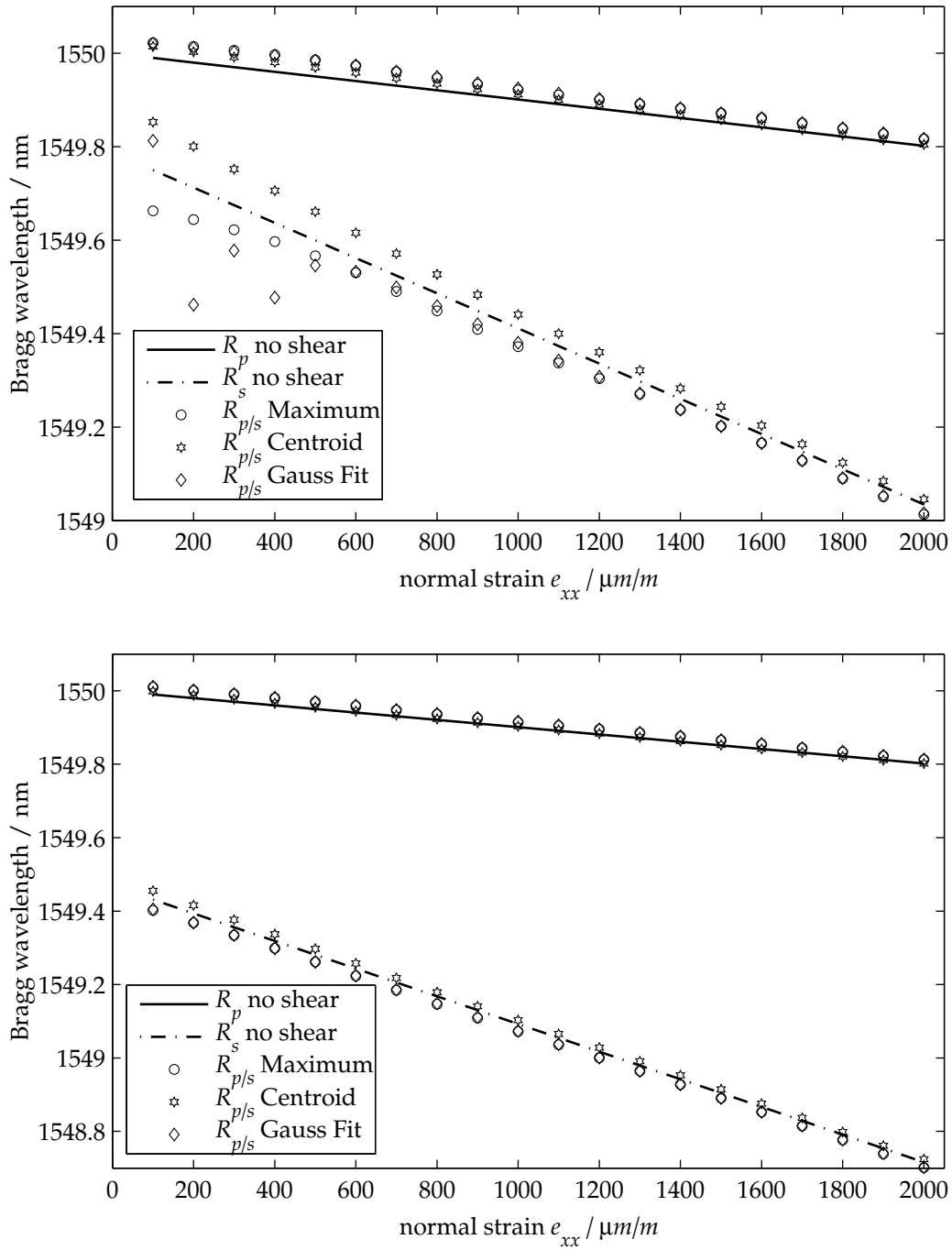


Figure 5. Computation of the Bragg wavelength of the s - and p -mode by three algorithms - maximum search, Gaussian fit and centroid. For comparison, the Bragg wavelength neglecting shear strain influences is computed. For symmetrical reflection peaks, all three algorithms yield the same result, therefore the result without shear is independent of the algorithm used. The upper figure simulates a fiber with a lower birefringence and a beat length of $L_B = 7.7$ mm. The lower figure corresponds to a fiber with a higher birefringence and a beat length of $L_B = 3,0$ mm.

is reduced and the effects are smaller. This may be observed by comparing the upper plot in figure 5 with the lower one in figure 5. Because of the higher birefringence, the reflection peaks of the polarization modes are stronger separated initially, leading to a different scaling of the plots.

The effect of polarization cross coupling will result in measurement error in the determination of the actual Bragg wavelength, since the spectral response becomes deformed. This interferes with the concept of multi-parameter strain sensing as suggested by Udd.¹⁴ The shear strain component e_{xy} has to be considered as an individual parameter, yielding a total of five parameters. These are $e_{xx}, e_{yy}, e_{xy}, e_{zz}$ and T . The four values extracted from the four Bragg peaks as suggested by Udd thus yield a singular problem.

4. CONCLUSION AND OUTLOOK

In this work we applied full tensor coupled mode theory to compute the optical response of a mechanically loaded fiber Bragg grating in a polarization maintaining fiber, when strong shear strains are present. We constructed a representative load case which may occur in a fiber sensing application. For several load values we calculated the output spectrum for the two polarization modes. We used this data to test three algorithms to determine the Bragg wavelength - maximum search, centroid and Gaussian fit. We showed how the algorithms perform for two different types of polarization maintaining fibers possessing different beat lengths. As expected we found the influence of shear strain to be reduced when fibers with high birefringence are employed. For a case of $L_B = 7.7$ mm, the deviations of the Bragg peak, caused by shear strain were found to be more than 100 μm .

Thus, a load case, which shows the same normal strains, but different shear strains may lead to strongly differing outputs. Comparing the values to a temperature measurement, the 100 μm would correspond to approximately 10°C or 100 $\mu\text{m}/\text{m}$. As a result this means, that shear strain has to be considered as a parameter influencing the output of a fiber Bragg grating measurement system. This has implications for the method of reconstructing the three normal strains and temperature as proposed by E. Udd.¹⁴ Since actually five parameters are influencing the spectral response significantly, the four parameters derived from the proposed experiment will not suffice to reconstruct the state of strain.

However, it may be observed, that the relative power of the polarization reflection peaks is strongly depending on the applied shear strain. It may therefore be possible to use this dependency to reconstruct a fifth parameter, possibly directly the shear strain component e_{xy} from the relative intensities of the two Bragg peaks. This would then allow to overcome the singularity of the problem and to again have a method at hand that allows the reconstruction of the full strain tensor by a single fiber Bragg grating sensor.

REFERENCES

1. J. Calero, S.-P. Wu, C. Pope, S. Chuang, and J. Murtha, "Theory and experiments on birefringent optical fibers embedded in concrete structures," *Journal of Lightwave Technology* **12**, p. 1081, 1994.
2. M. Prabugoud and K. Peters, "Finite element model for embedded fiber bragg grating sensor," *Smart Materials and Structures* **15**, p. 550, 2006.
3. M. McCall, "On the application of coupled mode theory for modeling fiber bragg gratings," *Journal of Lightwave Technology* **18**, p. 236, 2000.
4. T. Erdogan, "Fiber grating spectra," *Journal of Lightwave Technology* **15**, p. 1277, 1997.
5. T. Narasimhamutry, *Photoelastic and Electro-Optic Properties of Crystals*, Plenum Press, 1981.
6. M. S. Müller, L. Hoffmann, A. Sandmair, and A. W. Koch, "Full strain tensor treatment of fiber Bragg grating sensors," *IEEE Journal of Quantum Electronics* –, p. accepted for publication, 2008.
7. M. Müller, H. El-Khozondar, A. Bernardinia, and A. Koch, "Transfer matrix approach to four mode coupling in fiber bragg gratings," *IEEE Journal of Quantum Electronics* –, p. accepted for publication, 2009.
8. R. Ulrich and A. Simon, "Polarization optics of twisted single-mode fibers," *Applied Optics* **18**, p. 2241, 1979.
9. S. Rashleigh, W. Burns, R. Moeller, and R. Ulrich, "Polarization holding in birefringent single-mode fibers," *Optics Letters* **7**, p. 40, 1982.
10. R. Gafsi and M. El-Sherif, "Analysis of induced-birefringence effects on fiber bragg gratings," *Optical Fiber Technology* **6**, p. 299, 2000.
11. C. Lawrence, D. Nelson, E. Udd, and T. Bennett, "A fiber optic sensor for transverse strain measurement," *Experimental Mechanics* **39**(3), p. 202, 1999.
12. A. Ezbiri, S. Kanellopoulos, and V. Handerek, "High resolution instrumentation system for fibre-bragg grating aerospace sensors," *Optics Communications* **150**, pp. 43–48, 1998.
13. H. W. Lee and M. Song, "Fbg interrogation with a scanning fabry-perot filter and gaussian line-fitting algorithm," in *The 18th Annual Meeting of the IEEE Lasers and Electro-Optics Society*, 2005.
14. E. Udd, "Review of multi-parameter fiber grating sensors," in *Fiber Optic Sensors and Applications V, Proceedings of SPIE*, 2007.
15. T. Mawatari and D. Nelson, "A multi-parameter bragg grating fiber optic sensor and triaxial strain measurement," *Smart Materials and Structures* **17**, p. 19, 2008.
16. E. Chehura, C. Ye, S. Staines, S. James, and R. Tatam, "Characterization of the response of fibre bragg gratings fabricated in stress and geometrically induced high birefringent fibres to temperature and transverse load," *Smart Materials and Structures* **13**, p. 888, 2004.
17. C.-C. Ye, S. E. Staines, Stephen W James, and R. P. Tatam, "A polarization-maintaining fibre Bragg grating interrogation system for multi-axis strain sensing," *Measurement Science and Technology* **13**, p. 1446, 2002.
18. J. Noda, "Polarization-maintaining fibers and their applications," *Journal of Lightwave Technology* **LT-4**, pp. 1071–1089, 1986.
19. Y. Lo, J. Sirkis, and K. Ritchie, "A study of the optomechanical response of a diametrically loaded high-birefringent optical fiber," *Smart Materials and Structures* **4**, p. 327, 1995.
20. J. Zhao, X. Zhang, Y. Huang, and X. Ren, "Experimental analysis of birefringence effects on fiber bragg gratings induced by lateral compression," *Optics Communications* **229**, p. 203, 2003.